



Published in final edited form as:

Biochem Pharmacol. 2018 December ; 158: 298–304. doi:10.1016/j.bcp.2018.10.035.

## A power law function describes the time- and dose-dependency of V $\gamma$ 9V $\delta$ 2 T cell activation by phosphoantigens

Chia-Hung Christine Hsiao<sup>1</sup> and Andrew J. Wiemer<sup>1,2,\*</sup>

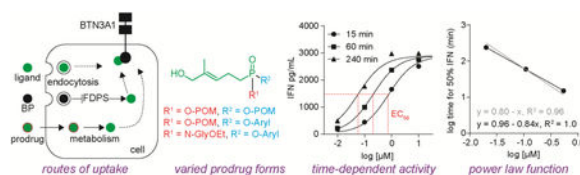
<sup>1</sup>Department of Pharmaceutical Sciences, University of Connecticut, Storrs, CT 06269, USA

<sup>2</sup>Institute for Systems Genomics, University of Connecticut, Storrs, CT 06269, USA

### Abstract

Phosphoantigens stimulate V $\gamma$ 9V $\delta$ 2 T cells after binding to BTN3A1 in target cells and cell-cell contact. We evaluated phosphoantigens including diphosphates, bisphosphonates, and prodrugs for ability to induce leukemia cells to stimulate V $\gamma$ 9V $\delta$ 2 T cell interferon- $\gamma$  secretion. Most compounds displayed time-dependent activity at exposure times between 15-240 minutes. Potency (EC<sub>50</sub> values) ranged between 8.4 nM and >100  $\mu$ M. The diphosphate C-HMBPP displayed a shallow dose-response slope (Hill slope = 0.71), while the bisphosphonate slopes were steep (Hill slopes >2), and the prodrugs intermediate. The bis-acyloxyalkyl POM<sub>2</sub>-C-HMBBP showed low nanomolar potency even at an exposure time of 1 minute. Mixed aryl-POM prodrugs also retained excellent potency at 15 minutes, while aryl-amidates were time dependent below 240 minutes. The sum of the dose and time logarithms is often constant, while a power law function fits most compounds. Collectively, these findings illustrate the exquisite activity of prodrugs relative to diphosphates and bisphosphonates.

### Graphical Abstract



### Keywords

CD277; gamma delta T cell; butyrophilin 3A1; BTN3A1; Haber's rule

\*Correspondence: Andrew J. Wiemer, University of Connecticut, 69 N Eagleville Road, Storrs, CT, 06269, Phone: 860.486.3966, Fax: 860.486.6857, andrew.wiemer@uconn.edu.

#### Disclosure

A.J.W. is a founder of Terpenoid Therapeutics. The current work did not involve the company.

**Publisher's Disclaimer:** This is a PDF file of an unedited manuscript that has been accepted for publication. As a service to our customers we are providing this early version of the manuscript. The manuscript will undergo copyediting, typesetting, and review of the resulting proof before it is published in its final citable form. Please note that during the production process errors may be discovered which could affect the content, and all legal disclaimers that apply to the journal pertain.

## 1. Introduction

T cells expressing the V $\gamma$ 9V $\delta$ 2 T cell receptor are prevalent in mucosa [1] and are the main population of  $\gamma\delta$  T cells in fetal [2] and adult [3] blood. These cells contribute to the immune response to pathogens [4] including *Mycobacterium tuberculosis* [5]. In contrast to traditional T cells that detect peptides, this non-traditional T cell population detects small diphosphates, known as phosphoantigens, produced by pathogens independent of the major histocompatibility complex. Because V $\gamma$ 9V $\delta$ 2 T cells also detect endogenous diphosphates, this cell type may also be involved in non-infectious diseases including cancer [6].

Natural phosphoantigens are intermediates of isoprenoid biosynthesis [7, 8]. These small and negatively charged diphosphates, such as (*E*)-4-hydroxy-3-methyl-but-2-enyl diphosphate (HMBPP) and isopentenyl diphosphate (IPP), bind to the intracellular domain of a transmembrane immunoglobulin known as butyrophilin 3A1 (BTN3A1) [9-15]. Binding to BTN3A1 induces a change to the conformation of the protein [9, 13, 16, 17], which can be detected extracellularly by cells expressing the V $\gamma$ 9V $\delta$ 2 T cell receptor (excellently reviewed in [18]). Once activated, these T cells perform a variety of effector functions [19].

Several groups are interested in potential clinical application of phosphoantigens, with one compound reaching clinical trials [20]. However, the charge of the natural diphosphates is a barrier to cellular uptake. Our approach has been to develop a library of novel phosphoantigen prodrugs as potential anti-cancer therapies [9, 21-23]. The prodrugs enhance uptake into cancer cells through utilization of bioactivatable, charge-neutral, phosphorous protecting groups [24]. Cells loaded with phosphoantigens then become targeted for destruction by the cytolytic activity of V $\gamma$ 9V $\delta$ 2 T cells, as well as stimulate the V $\gamma$ 9V $\delta$ 2 T cells to proliferate and to produce cytokines. These activities reduce viability and proliferation of the cancerous cells.

This prodrug approach has been also useful in understanding mechanisms underlying V $\gamma$ 9V $\delta$ 2 T cell activation. Prodrugs illustrated a role for internalization in the activity of phosphoantigens [25], and helped to develop the model of intracellular binding to BTN3A1 [9, 16]. Our library, which consists of a variety of prodrugs can provide a basis for understanding the uptake kinetics which may be of relevance to prodrug design not only of phosphoantigens but also of other drug candidates containing phosphorous. Here, we examine the relationship between cellular potency and uptake of phosphoantigens and their prodrugs. We specifically hypothesized that both phosphoantigen dose and cellular exposure time are critical to determining the potency and efficacy of the V $\gamma$ 9V $\delta$ 2 T cell interferon response.

## 2. Materials and Methods

### 2.1. Reagents

RPMI-1640, FBS, non-essential amino acids, pyruvate, penicillin streptomycin, HEPES, 2-mercaptoethanol, and lymphoprep were from Thermo Fisher Scientific (Pittsburgh, PA). IL-2 and the MACS  $\gamma\delta$  T cell negative selection kit were from Miltenyi Biotec (Bergisch Gladbach, Germany). K562 cells were from Sigma-Aldrich (St. Louis, MO) while Research

Blood Components (Boston, MA) supplied blood. The original passage number of the K562 cells is unknown, and K562 cells were maintained in suspension culture for no more than 3 months before thawing a new vial. Human interferon- $\gamma$  ELISA MAX deluxe kit was from Biolegend (San Diego, CA).

## 2.2. Test compounds

HMBPP (**1**) and C-HMBPP (**2**) were purchased from Echelon Biosciences (Salt Lake City, UT). Zoledronate (**3**) and risedronate (**4**) were purchased from Thermo Fisher Scientific. Compounds **5** and **6** [9], compound **7** [23], compound **8** [21], compounds **9** and **10** [22], and compounds **11-14** [26] were synthesized as previously described.

## 2.3. V $\gamma$ 9V $\delta$ 2 T cells

PBMCs from healthy donors were isolated from heparinized buffy coat using Lymphoprep. PBMCs were resuspended at  $2-4 \times 10^6$  cells/mL in fresh T cell media (RPMI-1640, 10% heat-inactivated FBS, 1x HEPES, pyruvate, NEAA, and 2-mercaptoethanol). Cells were stimulated with 10 nM HMBPP for 72 hours and cultured for another 11 days. Fresh IL-2 (5 ng/mL) was provided every 3 days. After 12-14 days, V $\gamma$ 9V $\delta$ 2 T cells were purified by negative selection.

## 2.4. Interferon- $\gamma$ ELISA

K562 cells were cultured in T cell media and maintained below  $1 \times 10^6$  cells per mL. K562 cells were suspended in media and were treated with test compounds. K562 cells were washed twice in experiments involving prodrugs or bisphosphonates and five times in experiments involving HMBPP or C-HMBPP. The wash steps were performed in 0.2 mL tubes with  $\sim 150$   $\mu$ L media, spun for 20 seconds in a benchtop centrifuge with strip tube adaptor, and the media was aspirated from the cell pellet. We expected HMBPP and C-HMBPP to require more wash steps due to their potency, shallow slope, and slow uptake, and prior experiments determined five wash steps were sufficient to reduce activity of HMBPP in BTN3A1 knockout cells to background [16]. A pilot experiment with varied wash numbers showed that more than two wash steps was not necessary for bisphosphonates and prodrugs. Twenty  $\mu$ L of the washed cells were diluted into T cells at a ratio of 3:1 (T cells: K562 cells) in 200  $\mu$ L in duplicate, resulting in 4,000 K562 cells and 12,000 effector T cells per well. Mixtures were incubated for 20 hours, following which interferon- $\gamma$  was assessed by ELISA. Experimental values fell within the range of a standard curve. Concentrations in dose response experiments were determined in an initial range finding experiment, and chosen to cover the range from zero effect to maximal effect when possible.

## 2.5 Statistics

Experiments were performed at least three times using at least two donors. Graphs were constructed and data analyzed using GraphPad Prism 6. Dose response curves were analyzed using a log (agonist) versus response -- variable slope (four parameters) model in which the top, bottom, and Hill slope parameters were assigned as shared values within each compound. EC<sub>50</sub> values for each time point were calculated, and the EC<sub>50</sub> with 95% confidence intervals, the Hill slope, and R<sup>2</sup> values reported in Table 1. Log EC<sub>50</sub> values for

each compound and time point were plotted on the X-axis versus  $\log t$  on the Y-axis (log time for 50% interferon- $\gamma$  response). Power constants ( $k_1$ ) were calculated according to the formula  $k_1 = \log t + a \log C$  where  $C$  is the concentration ( $\mu\text{M}$ ) and  $t$  the incubation time (min), and both  $a$  and  $k$  were variables. The fit ( $R^2$ ) was assessed for each compound. Additive constants ( $k_2$ ) were calculated using  $a = 1$  to solve for an initial  $k_2$  value for each compound, then the fit ( $R^2$ ) was assessed using the calculated  $k_2$  value and  $a = 1$  [27].

### 3. Results

#### 3.1. POM2-C-HMBP stimulates V $\gamma$ 9V $\delta$ 2 T cell interferon- $\gamma$ .

We compared three classes of phosphoantigens (Figure 1) for their ability to stimulate V $\gamma$ 9V $\delta$ 2 T cells (Figure 2A). HMBPP (**1**) is the most potent natural phosphoantigen (72 hour PBMC expansion  $EC_{50} = 0.50$  nM [9]) and is the prototypical agonist [7]. Zoledronate (**3**) (72 hour PBMC expansion  $EC_{50} = 900$  nM) is a bisphosphonate which acts indirectly by inhibiting the enzyme farnesyl diphosphate synthase (FDPS) and increasing cellular prenyl diphosphates [28]. POM2-C-HMBP (**5**) (72 hour expansion  $EC_{50} = 5.4$  nM [9]) is a prodrug that delivers the phosphoantigen intracellularly [9]. Charged zoledronate and HMBPP are internalized via energy dependent uptake mechanisms [25, 29], while both POM<sub>2</sub>-C-HMBP and zoledronate are dependent upon cellular enzymes for activity (Figure 2B).

Compounds were tested for their ability to promote a V $\gamma$ 9V $\delta$ 2 T cell response to pre-treated K562 cells. Because both cell types in this co-culture express BTN3A1, we pre-loaded and washed the K562 cells prior to exposure to the T cells (Figure 2A). In this way, the T cells are activated only if the K562 loading results in detectable changes to cell surface BTN3A1. We tested HMBPP, zoledronate, and POM2-C-HMBP for their ability to promote interferon- $\gamma$ , the predominant V $\gamma$ 9V $\delta$ 2 T cell cytokine. K562 cells were treated for 60 minutes at 1  $\mu\text{M}$ , washed, and exposed to purified primary V $\gamma$ 9V $\delta$ 2 T cells for 20 hours (Figure 2C). No measurable effect of zoledronate was observed, while HMBPP treatment induced a mild response. In contrast, POM<sub>2</sub>-C-HMBP promoted high interferon- $\gamma$ . Therefore, under conditions of limited uptake, POM<sub>2</sub>-C-HMBP but not HMBPP or zoledronate markedly promotes V $\gamma$ 9V $\delta$ 2 T cell interferon- $\gamma$  production. This is in contrast to the 72 hour proliferation assay, in which HMBPP is approximately ten fold more potent than POM<sub>2</sub>-C-HMBP [9], and zoledronate is active at high nano molar concentrations.

#### 3.2. Rapid activity of phosphoantigen prodrugs relative to bisphosphonates and diphosphates.

To further assess zoledronate (**3**) and risedronate (**4**), we performed dose response experiments (Figure 3A/B). Importantly, the curves were generated at varying times- 15, 60, or 240 minutes. The  $EC_{50}$  values are presented in Table 1, and were in the mid-micromolar range. The potency of zoledronate and risedronate was similar, as expected due to their similar inhibition of FDPS [30]. Both compounds showed relatively large differences (greater than 3-4 fold) in potency depending on the exposure time, indicative of slow uptake, and perhaps longer times are needed to reach intracellular levels needed for FDPS inhibition and accumulation of IPP. The dose response slope (Hill Slope) of both compounds was steep ( 2).

We next assessed POM<sub>2</sub>-C-HMBP (Figure 3C). We found less than 2 fold difference between the EC<sub>50</sub> values at 15 and 240 minutes. POM<sub>2</sub>-C-HMBP (**5**) is more potent than zoledronate (**3**), while the time dependency of POM<sub>2</sub>-C-HMBP is lower. We repeated the experiment using shorter incubation times (Figure 3D), where the differences between the time points were more pronounced, though POM<sub>2</sub>-C-HMBP achieved an EC<sub>50</sub> of 110 nM with only 1 minute of exposure, indicative of rapid cellular activation.

HMBPP (**1**) and the closely related C-HMBPP (**2**) require energy dependent cellular uptake, and despite their high potency during long exposures, are less active during short exposures [25]. To more fully characterize this phenomenon, we applied our assay conditions to HMBPP. Due to the difference in HMBPP potency between short and long exposure times, excessive washing is required to minimize the effect of residual HMBPP. Previously we noted that 5 wash steps was sufficient to reduce HMBPP treated BTN-deficient cells to background [16]. Here we treated K562 cells with HMBPP at the indicated doses and times, washed 5 times, and characterized (Figure 3E). Notably, despite its potency, HMBPP was unable to maximally activate K562 cells in the four hour timeframe. No time dependency was observed with HMBPP in these assays, supporting the idea put forth by others that it can be pulsed into cells [31], though interpretation is complicated by inability to reach a maximal effect. Compound **5**, used as a positive control at 1 μM for 60 minutes, still retained maximal activity despite additional washing. In contrast, C-HMBPP did plateau (Figure 3F), indicating the inability of HMBPP to plateau was related to the cellular instability of the diphosphate. C-HMBPP displayed a shallow Hill slope, similar as HMBPP in other assays [21], and a high time dependency.

We next assessed mono-acyloxyalkyl-mono-methyl prodrugs. The methyl group is thought to reduce charge and enable cell permeability, but to be metabolically stable, allowing assessment of the impact of a single acyloxyalkyl protecting group. Relative to compound **5**, compound **6** [9] displayed both reduced potency and increased time dependency, while compound **7** [23] displayed similar potency and time dependency to compound **6** (Table 1). The tris-POM prodrug **8** [21] showed similar time dependency as compound **5**, though the potency of **8** was lower than **5** (Table 1). Taken together, prodrugs containing entirely two or three pivaloyloxymethyl groups can be rapidly activated, but the presence of a single methyl protecting group reduces both potency and speed of activation.

### 3.3. Comparison of mixed aryl-POM and aryl-amidate prodrugs.

Recently, there has been much excitement about aryl-amidates, in part due to the clinical success of sofosbuvir [32]. We reported a series of novel aryl-POM prodrugs [22] and a series of aryl-amide prodrugs [26]. Three of the aryl-POM prodrugs (**9-11**) were evaluated (Figure 4A/B/C). Much like the bis- and tris-POM prodrugs, the aryl-POM prodrugs **9-11** display excellent potency (4 hour EC<sub>50</sub> values between 8.4 nM and 18 nM) and rapid cell activation (only 3 fold difference between the 15 minute and 240 minute exposures). Similarly, the aryl-amidate prodrugs **12-14** also displayed excellent potency after four hours of K562 cell exposure (Figure 4D/E/F), with EC<sub>50</sub> values between 20 to 56 nM. However, their activation rate is slower than the aryl-POM or bis-/tris-POM compounds, with over a

13 fold difference between the 15 minute and 240 minute exposures. The slopes of all six compounds **9-14** were slightly below 1, ranging from 0.83 to 1.0 (Table 1).

#### 3.4. Phosphoantigens and their prodrugs display similar maximal activation.

Thirteen of the fourteen compounds tested (all but HMBPP) reached maximal activity following 4 hours of exposure, as determined both by a plateau at the high end of the dose response curve as well as never exceeding the activity of POM<sub>2</sub>-C-HMBP (**5**). To directly assess whether any of the compounds or prodrugs differed in maximal efficacy, we picked maximal concentrations of each compound based on the dose response curves at 4 hours, and tested them side-by-side against V $\gamma$ 9V $\delta$ 2 T cells from the same three donors. No statistically-significant differences were observed between compounds **2-8** (Figure 5A). A second round of testing again showed no statistically-significant differences between compounds **5** and **9-14** (Figure 5B). Together, none of the phosphoantigens tested differed in their maximal effect, nor did any of the prodrugs.

Although our experiments were not designed to assess donor variability, some differences were noted. Occasionally PBMCs failed to expand with HMBPP. However, we cannot determine that this is due to lack of HMBPP sensitivity instead of a lower initial frequency of V $\gamma$ 9V $\delta$ 2 T cells or another factor. All donors that were expandable responded quite similarly upon exposure to the loaded K562 cells, with maximal stimulation typically around 3000 pg/mL independent of donor.

#### 3.5. Relationship between potency and activation kinetics.

There is a clear relationship between cellular potency and time of exposure to compounds, which varies between direct BTN3A1 ligands and indirect acting compounds, between charged compounds and prodrugs, and even between different prodrugs. We were curious to see whether there was a constant relationship between the concentration  $C$  and exposure time  $t$ . Excluding HMBPP, which did not reach a maximal effect, we assessed the concentration required at each time to reach 50% of the maximal interferon- $\gamma$  response. All of the compounds fit well to a simple power law function  $\log t + \alpha \log C = k_1$  (average  $R^2 = 0.96$ ) (Table 1). Surprisingly, over half (7/13) of the compounds fit the more straightforward  $\log t + \log C = k_2$  relationship with  $R^2$  values above 0.90, and the average  $R^2$  for the entire set was 0.80. Representative plots for zoledronate (**3**) and compound **13** are shown (Figure 5C/D). Taken together, the half-maximal phosphoantigen response can be readily calculated as a function of both concentration and exposure time.

Notably, the two highest  $k$  values were observed with the bisphosphonates, zoledronate (**3**) and risedronate (**4**) ( $k_2 = 3.6$  and  $4.1$ , respectively). Likewise, C-HMBPP (**2**) displayed a  $k_2 = 2.1$ . In contrast, POM<sub>2</sub>-C-HMBP **5** displayed a lower  $k_2 = 0.28$ . When both dose and time are taken into account, the activity is  $\sim 4$  log units stronger than that of the bisphosphonates and  $\sim 2$  log units stronger than C-HMBPP. The mixed aryl-POM compounds were similarly active, including the most active compound (**9**), while the aryl-amidates display intermediate activity. Because potency is dependent upon exposure time, comparison of these constants is a better approach than simple comparisons of EC<sub>50</sub> values, with the lower values representing more efficient activation.

## 4. Discussion

The findings of our study are relevant to the pre-clinical development of phosphoantigens. The metabolically stable bisphosphonate drugs have been proposed as an alternative strategy for activation of V $\gamma$ 9V $\delta$ 2 T cells [33], and their activity correlates with FDPS inhibition [28]. These studies were performed at a single time point of sixteen hours with continuous bisphosphonate exposure. However, bisphosphonates also cause cellular toxicity related to inhibition of FDPS. Additionally, bisphosphonates display rapid bone sequestration in vivo [34], further complicating their use as phosphoantigens. The pulse bisphosphonate approach has been proposed to minimize the toxicity [33], and indeed in our hands pulsing with bisphosphonate appears to be a better option than pulsing with diphosphate phosphoantigens, because the bisphosphonate pulse can maximally activate the V $\gamma$ 9V $\delta$ 2 T cells even after a short exposure. This does require high bisphosphonate concentration.

The prodrug approach is adventitious relative to both the diphosphate and bisphosphonate phosphoantigens. Compared to the diphosphates, the speed of activation of the prodrugs is much faster, happening in minutes. The prodrugs also take advantage of the enhanced stability of the phosphonate, are active at lower concentrations, and avoid the mechanism-based toxicity and substructure based bone distribution of the bisphosphonate phosphoantigens.

We compared activity of varied prodrugs intended to deliver the same ligand, C-HMBP [35]. Because the ligand is constant, differences are due to metabolism. The bis-POM 5 was among the most active, though it did not fit well to the log-additive model in the range of 15-240 minutes. The log-additive fit was improved with exposure under 16 minutes ( $R^2$  of 0.70 versus 0.37). We cannot say if even shorter exposure (<1 min) would produce a better fit, because the time required to process these samples precludes assays of this duration. The aryl-POM prodrugs **9-11** were similar to the bis-POM compound in this assay. In contrast, the aryl-amidate prodrugs **12-14** were all an order of magnitude less active, though their activity fit much better to the log-additive model ( $R^2$  values all above 0.94). As exposure time increased, both the aryl-POM and aryl-amidate compounds converged to a maximal potency in the low nanomolar range. It is unclear whether the cellular activity gains of the aryl-POM strategy relative to the aryl-amidate strategy would benefit in vivo applications, though this point merits further study.

The Hill slope can be an important measure of drug response related to mechanism [36, 37]. In general, systems with multiple binding sites in which binding of one ligand increases binding of subsequent ligands are considered positively cooperative and demonstrate steep Hill slopes, while those in which binding of one ligand decreases binding of subsequent ligands are considered negatively cooperative and exhibit shallow Hill slopes. We previously identified shallow slopes for HMBPP [21], and our data here is not inconsistent, though without reaching maximal activity it was not possible to accurately quantify the Hill slope of HMBPP. C-HMBPP also exhibits a shallow slope, while reaching full efficacy. The shallow Hill slope is consistent with a model of negative cooperativity at the cellular level, though it can also result from other factors [21], and negative cooperativity does not necessarily show up in a Hill slope [36, 38]. BTN3A1 has been suggested to exist as either a heterodimer or

homodimer with two ligand binding sites [39]. Therefore, the potential for cooperativity in its activation exists. To assess the potential for cooperativity, we determined the Hill slopes for each compound (Table 1). In contrast to C-HMBPP, both bisphosphonates showed steep Hill slopes, perhaps suggestive of positive cooperativity related to inhibition of FDPS and accumulation of endogenous prenyl diphosphates. Taken together, under time restricted conditions, we continue to propose that diphosphate phosphoantigens display Hill slopes consistent with negative cooperativity, though further studies directed specifically at phosphoantigen cooperativity would aid in our understanding of this phenomena.

In clinical trials with BrHPP, low plasma stability was reported with the plasma half-life under 10 minutes [20]. Use of diphosphates such as BrHPP required continuous IV dosing, while in pre-clinical animal studies HMBPP required IM injection [40]. In light of our data, diphosphates also would be expected to be poor drug candidates with respect to their slow internalization and low cellular stability [25, 31]. In fact, despite HMBPP being the natural BTN3A1 ligand [10], it was not able to induce a maximal response with exposure times below 4 hours. In contrast, C-HMBPP, which contains a metabolically stable phosphonate [35], was able to produce maximal activation, even with only 15 minutes exposure. From a pre-clinical development standpoint, this data demonstrates a clear advantage of phosphonate containing ligands, which is not obvious in experiments performed with longer exposure times.

Finally, it remains to be determined how phosphoantigens may ultimately find clinical use for cancer therapy. For example, one could imagine them being injected locally into the site of the tumor to encourage activation of V $\gamma$ 9V $\delta$ 2 T cells at a specific location or perhaps even targeted specifically to malignant cells to encourage their attack. Although our current study did not examine the issues of tissue specificity or malignant versus normal specificity, in the long run it may be possible to design varied prodrug forms to achieve cell type specificity in addition to controlling the rate of cellular activation. We did not examine the potential role of immune coreceptors in conferring sensitivity or resistance to various phosphoantigens, though it is possible they may impact the response. Further studies are necessary to fully understand these issues and how the prodrugs may function in an in vivo setting to achieve specificity.

## Acknowledgments

Compounds were provided by Prof. Rocky Barney, Dr. Rebekah Shippy, Ben Foust, Nick Lentini, and Prof. David Wiemer at the University of Iowa. Assistance with cell culture from Jin Li and Sherry Agabiti is appreciated. Research reported in this publication was supported by the National Cancer Institute of the United States National Institutes of Health under Award Number R01CA186935 (A.J.W., P.I.) and the Herman Frasch Foundation for Chemical Research, Bank of America, N.A., Trustee (HF17) (A.J.W., PI).

## References

1. McCarthy NE, Eberl M. Human gammadelta T-Cell Control of Mucosal Immunity and Inflammation. *Front Immunol* 2018; 9: 985. [PubMed: 29867962]
2. Dimova T, Brouwer M, Gosselin F, Tassignon J, Leo O, Donner C, et al. Effector Vgamma9Vdelta2 T cells dominate the human fetal gammadelta T-cell repertoire. *Proc Natl Acad Sci U S A* 2015; 112(6): E556–65. [PubMed: 25617367]



3. Parker CM, Groh V, Band H, Porcelli SA, Morita C, Fabbi M, et al. Evidence for extrathymic changes in the T cell receptor gamma/delta repertoire. *J Exp Med* 1990; 171(5): 1597–612. [PubMed: 2185330]
4. Hintz M, Reichenberg A, Altincicek B, Bahr U, Gschwind RM, Kollas AK, et al. Identification of (E)-4-hydroxy-3-methyl-but-2-enyl pyrophosphate as a major activator for human gammadelta T cells in *Escherichia coli*. *FEBS Lett* 2001; 509(2): 317–22. [PubMed: 11741609]
5. Qaqish A, Huang D, Chen CY, Zhang Z, Wang R, Li S, et al. Adoptive Transfer of Phosphoantigen-Specific gammadelta T Cell Subset Attenuates Mycobacterium tuberculosis Infection in Nonhuman Primates. *J Immunol* 2017; 198(12): 4753–4763. [PubMed: 28526681]
6. Riganti C, Massaia M, Davey MS, Eberl M. Human gammadelta T-cell responses in infection and immunotherapy: common mechanisms, common mediators? *Eur J Immunol* 2012; 42(7): 1668–76. [PubMed: 22806069]
7. Morita CT, Jin C, Sarikonda G, Wang H. Nonpeptide antigens, presentation mechanisms, and immunological memory of human Vgamma2Vdelta2 T cells: discriminating friend from foe through the recognition of prenyl pyrophosphate antigens. *Immunol Rev* 2007; 215: 59–76. [PubMed: 17291279]
8. Wiemer AJ, Hsiao CH, Wiemer DF. Isoprenoid metabolism as a therapeutic target in gram-negative pathogens. *Curr Top Med Chem* 2010; 10(18): 1858–71. [PubMed: 20615187]
9. Hsiao CH, Lin X, Barney RJ, Shippy RR, Li J, Vinogradova O, et al. Synthesis of a phosphoantigen prodrug that potently activates Vgamma9Vdelta2 T-lymphocytes. *Chem Biol* 2014; 21(8): 945–54. [PubMed: 25065532]
10. Sandstrom A, Peigne CM, Leger A, Crooks JE, Konczak F, Gesnel MC, et al. The intracellular B30.2 domain of butyrophilin 3A1 binds phosphoantigens to mediate activation of human Vgamma9Vdelta2 T cells. *Immunity* 2014; 40(4): 490–500. [PubMed: 24703779]
11. Rhodes DA, Chen HC, Price AJ, Keeble AH, Davey MS, James LC, et al. Activation of human gammadelta T cells by cytosolic interactions of BTN3A1 with soluble phosphoantigens and the cytoskeletal adaptor perioplakin. *J Immunol* 2015; 194(5): 2390–8. [PubMed: 25637025]
12. Wang H, Morita CT. Sensor Function for Butyrophilin 3A1 in Prenyl Pyrophosphate Stimulation of Human Vgamma2Vdelta2 T Cells. *J Immunol* 2015; 195(10): 4583–94. [PubMed: 26475929]
13. Salim M, Knowles TJ, Baker AT, Davey MS, Jeeves M, Sridhar P, et al. BTN3A1 Discriminates gammadelta T Cell Phosphoantigens from Nonantigenic Small Molecules via a Conformational Sensor in Its B30.2 Domain. *ACS Chem Biol* 2017; 12(10): 2631–2643. [PubMed: 28862425]
14. Riano F, Karunakaran MM, Starick L, Li J, Scholz CJ, Kunzmann V, et al. Vgamma9Vdelta2 TCR-activation by phosphorylated antigens requires butyrophilin 3 A1 (BTN3A1) and additional genes on human chromosome 6. *Eur J Immunol* 2014; 44(9): 2571–6. [PubMed: 24890657]
15. Harly C, Guillaume Y, Nedellec S, Peigne CM, Monkkonen H, Monkkonen J, et al. Key implication of CD277/butyrophilin-3 (BTN3A) in cellular stress sensing by a major human gammadelta T-cell subset. *Blood* 2012; 120(11): 2269–79. [PubMed: 22767497]
16. Nguyen K, Li J, Puthenveetil R, Lin X, Poe MM, Hsiao CC, et al. The butyrophilin 3A1 intracellular domain undergoes a conformational change involving the juxtamembrane region. *FASEB J* 2017; 31(11): 4697–4706. [PubMed: 28705810]
17. Starick L, Riano F, Karunakaran MM, Kunzmann V, Li J, Kreiss M, et al. Butyrophilin 3A (BTN3A, CD277)-specific antibody 20.1 differentially activates Vgamma9Vdelta2 TCR clonotypes and interferes with phosphoantigen activation. *Eur J Immunol* 2017; 47(6): 982–992. [PubMed: 28386905]
18. Boutin L, Scotet E. Towards Deciphering the Hidden Mechanisms That Contribute to the Antigenic Activation Process of Human Vgamma9Vdelta2 T Cells. *Front Immunol* 2018; 9(828): 828. [PubMed: 29731756]
19. Vantourout P, Hayday A. Six-of-the-best: unique contributions of gammadelta T cells to immunology. *Nat Rev Immunol* 2013; 13(2): 88–100. [PubMed: 23348415]
20. Fournie JJ, Sicard H, Poupot M, Bezombes C, Blanc A, Romagne F, et al. What lessons can be learned from gammadelta T cell-based cancer immunotherapy trials? *Cell Mol Immunol* 2013; 10(1): 35–41. [PubMed: 23241899]

21. Shippy RR, Lin X, Agabiti SS, Li J, Zangari BM, Foust BJ, et al. Phosphinophosphonates and Their Tris-pivaloyloxymethyl Prodrugs Reveal a Negatively Cooperative Butyrophilin Activation Mechanism. *J Med Chem* 2017; 60(6): 2373–2382. [PubMed: 28218845]
22. Foust BJ, Poe MM, Lentini NA, Hsiao CC, Wiemer AJ, Wiemer DF. Mixed Aryl Phosphonate Prodrugs of a Butyrophilin Ligand. *ACS Med Chem Lett* 2017; 8(9): 914–918. [PubMed: 28947936]
23. Wiemer AJ, Shippy RR, Kilcollins AM, Li J, Hsiao CH, Barney RJ, et al. Evaluation of a 7-Methoxycoumarin-3-carboxylic Acid Ester Derivative as a Fluorescent, Cell-Cleavable, Phosphonate Protecting Group. *Chembiochem* 2016; 17(1): 52–5. [PubMed: 26503489]
24. Wiemer AJ, Wiemer DF. Prodrugs of phosphonates and phosphates: crossing the membrane barrier. *Top Curr Chem* 2015; 360: 115–60. [PubMed: 25391982]
25. Kilcollins AM, Li J, Hsiao CH, Wiemer AJ. HMBPP Analog Prodrugs Bypass Energy-Dependent Uptake To Promote Efficient BTN3A1-Mediated Malignant Cell Lysis by Vgamma9Vdelta2 T Lymphocyte Effectors. *J Immunol* 2016; 197(2): 419–28. [PubMed: 27271567]
26. Lentini NA, Foust BJ, Hsiao CC, Wiemer AJ, Wiemer DF. Phosphoramidate Prodrugs of a Butyrophilin Ligand Display Plasma Stability and Potent Vgamma9 Vdelta2 T Cell Stimulation. *J Med Chem* 2018.
27. Miller FJ, Schlosser PM, Janszen DB. Haber's rule: a special case in a family of curves relating concentration and duration of exposure to a fixed level of response for a given endpoint. *Toxicology* 2000; 149(1): 21–34. [PubMed: 10963858]
28. Sanders JM, Ghosh S, Chan JM, Meints G, Wang H, Raker AM, et al. Quantitative structure-activity relationships for gammadelta T cell activation by bisphosphonates. *J Med Chem* 2004; 47(2): 375–84. [PubMed: 14711309]
29. Thompson K, Rogers MJ, Coxon FP, Crockett JC. Cytosolic entry of bisphosphonate drugs requires acidification of vesicles after fluid-phase endocytosis. *Mol Pharmacol* 2006; 69(5): 1624–32. [PubMed: 16501031]
30. Ebetino FH, Hogan AM, Sun S, Tsoumpra MK, Duan X, Triffitt JT, et al. The relationship between the chemistry and biological activity of the bisphosphonates. *Bone* 2011; 49(1): 20–33. [PubMed: 21497677]
31. Wang H, Sarikonda G, Puan KJ, Tanaka Y, Feng J, Giner JL, et al. Indirect stimulation of human Vgamma2Vdelta2 T cells through alterations in isoprenoid metabolism. *J Immunol* 2011; 187(10): 5099–113. [PubMed: 22013129]
32. Sofia MJ, Chang W, Furman PA, Mosley RT, Ross BS. Nucleoside, nucleotide, and non-nucleoside inhibitors of hepatitis C virus NS5B RNA-dependent RNA-polymerase. *J Med Chem* 2012; 55(6): 2481–531. [PubMed: 22185586]
33. Nada MH, Wang H, Workalemahu G, Tanaka Y, Morita CT. Enhancing adoptive cancer immunotherapy with Vgamma2Vdelta2 T cells through pulse zoledronate stimulation. *J Immunother Cancer* 2017; 5: 9. [PubMed: 28239463]
34. Roelofs AJ, Stewart CA, Sun S, Blazewska KM, Kashemirov BA, McKenna CE, et al. Influence of bone affinity on the skeletal distribution of fluorescently labeled bisphosphonates in vivo. *J Bone Miner Res* 2012; 27(4): 835–47. [PubMed: 22228189]
35. Boedec A, Sicard H, Dessolin J, Herbette G, Ingoure S, Raymond C, et al. Synthesis and biological activity of phosphonate analogues and geometric isomers of the highly potent phosphoantigen (E)-1-hydroxy-2-methylbut-2-enyl 4-diphosphate. *J Med Chem* 2008; 51(6): 1747–54. [PubMed: 18303828]
36. Fallahi-Sichani M, Honarnejad S, Heiser LM, Gray JW, Sorger PK. Metrics other than potency reveal systematic variation in responses to cancer drugs. *Nat Chem Biol* 2013; 9(11): 708–14. [PubMed: 24013279]
37. Jenkins JL. Drug discovery: Rethinking cellular drug response. *Nat Chem Biol* 2013; 9(11): 669–70. [PubMed: 24141220]
38. Weiss JN. The Hill equation revisited: uses and misuses. *FASEB J* 1997; 11(11): 835–41. [PubMed: 9285481]
39. Gu S, Borowska MT, Boughter CT, Adams EJ. Butyrophilin3A proteins and Vgamma9Vdelta2 T cell activation. *Semin Cell Dev Biol* 2018.

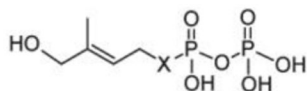
40. Ali Z, Shao L, Halliday L, Reichenberg A, Hintz M, Jomaa H, et al. Prolonged (E)-4-hydroxy-3-methyl-but-2-enyl pyrophosphate-driven antimicrobial and cytotoxic responses of pulmonary and systemic Vgamma2Vdelta2 T cells in macaques. *J Immunol* 2007; 179(12): 8287–96. [PubMed: 18056373]

Author Manuscript

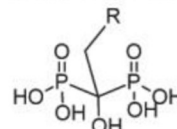
Author Manuscript

Author Manuscript

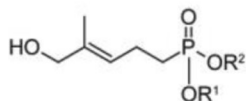
Author Manuscript

Direct Ligands

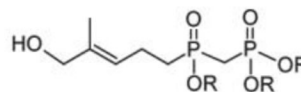
X = O, HMBPP (1)  
X = CH<sub>2</sub>, C-HMBPP (2)

Bisphosphonates

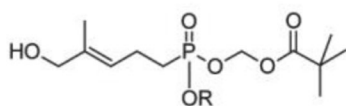
R = imidazol-1-yl, zoledronate (3)  
R = pyridin-3-yl, risedronate (4)

Phosphoantigen Prodrugs

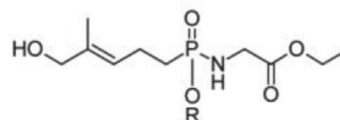
R<sup>1</sup> = R<sup>2</sup> = POM (5)  
R<sup>1</sup> = Me, R<sup>2</sup> = POM (6)  
R<sup>1</sup> = Me, R<sup>2</sup> = CCOM (7)



R = POM (8)



R = phenyl (9)  
R = 1-naphthyl (10)  
R = 2-naphthyl (11)



R = phenyl (12)  
R = 1-naphthyl (13)  
R = 2-naphthyl (14)

**Figure 1. Structures of compounds.**

POM = pivaloyloxymethyl, CCOM = coumarin-carboxylate oxymethyl.

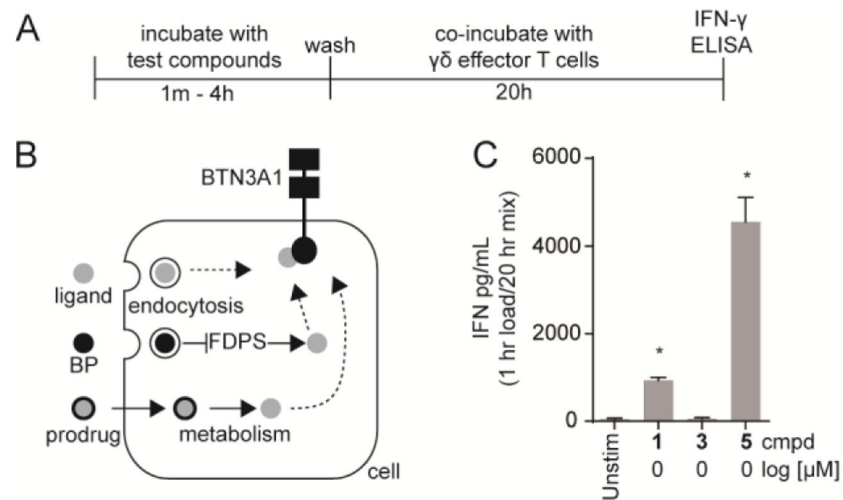


**Figure 2. K562 cells pre-loaded with a phosphoantigen prodrug stimulate V $\gamma$ 9V $\delta$ 2 T cell interferon- $\gamma$  production more potently than a natural BTN3A1 ligand or a bisphosphonate drug.** A) Timeline for compound exposure to target cells and target cell exposure to effector V $\gamma$ 9V $\delta$ 2 T cells. B) Compounds in this study act as either direct BTN3A1 ligands, prodrugs requiring cellular metabolic activation, or indirect bisphosphonates (BPs) which require FDPS inhibition. C) Stimulation of V $\gamma$ 9V $\delta$ 2 T cell interferon- $\gamma$  by K562 cells pre-exposed to compounds for equivalent time (60 minutes) and concentration (1  $\mu$ M). Bars represent means and standard deviations of three independent experiments (n=3). Statistical significance was determined by oneway ANOVA with Tukey's post-hoc analysis. \*p < 0.05 versus untreated control.

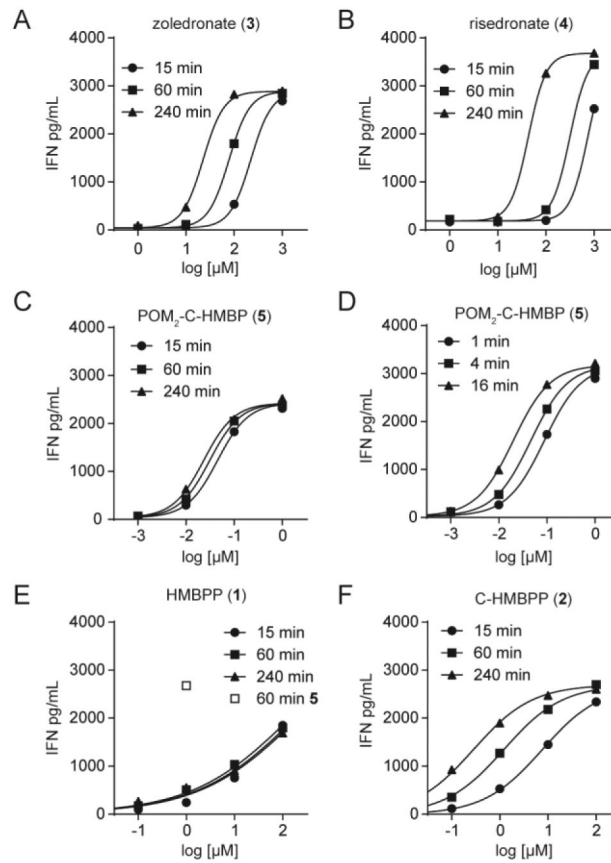


**Figure 3. Dose- and time- dependent activation of V $\gamma$ 9V $\delta$ 2 T cells by bisphosphonates, diphosphates and phosphoantigen POM<sub>2</sub>-C-HMBP.** Interferon- $\gamma$  response of V $\gamma$ 9V $\delta$ 2 T cells after K562 cell exposure to compounds for varied time points.

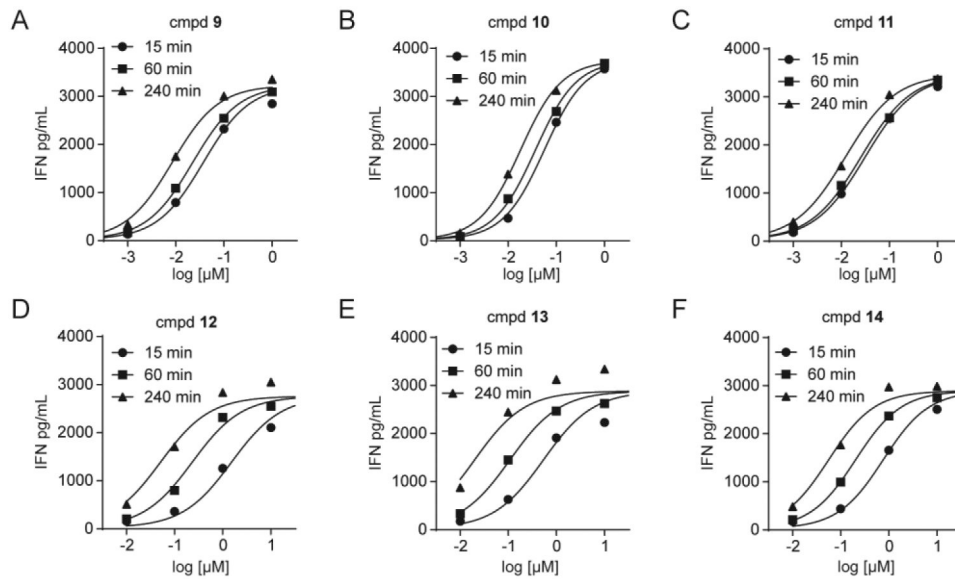


**Figure 4. Mixed aryl acyloxyalkyl and aryl amidate prodrugs stimulate V $\gamma$ 9V $\delta$ 2 T cell interferon- $\gamma$  production with high potency but vary in activation kinetics.** Interferon- $\gamma$  response of V $\gamma$ 9V $\delta$ 2 T cells after K562 cell exposure to compounds for varied time points.

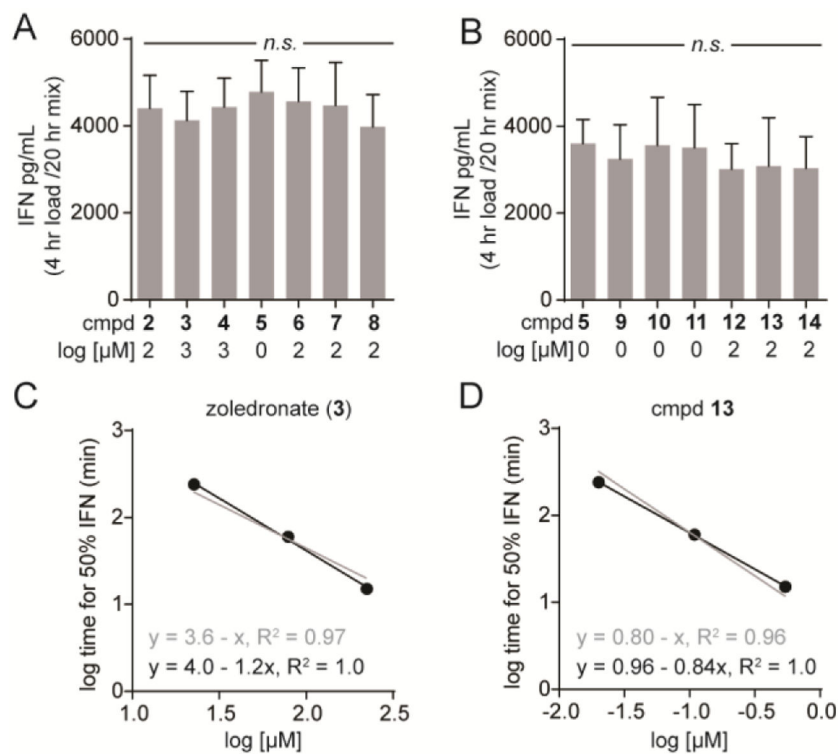


**Figure 5. Test compounds produce similar maximal interferon- $\gamma$  response and many fit a log-additive model.**

A-B) The maximal effect of A) compounds **2-8** and B) compounds **9-14**. Concentrations for each compound were determined based on pilot dose response curves and are indicated. Exposure time was 4 hours. Compound **5** was repeated as a positive control in the latter set. Bars represent means and standard deviations of three independent experiments ( $n=3$ ). Statistical significance was determined by one-way ANOVA with Tukey's post-hoc analysis. C-D) The graphs for C) zoledronate and D) compound **13** compare the log-additive plot (grey lines) to the power law plot (black lines) for the time to 50% maximal interferon- $\gamma$  response for each compound.



Table 1.

Compound characteristics for V $\gamma$ 9V $\delta$ 2 T cell IFN- $\gamma$  production by pre-loaded K562 cells

cmpd (n=3)	15 min EC <sub>50</sub> [ $\mu$ M] (95% CI)	60 min EC <sub>50</sub> [ $\mu$ M] (95% CI)	240 min EC <sub>50</sub> [ $\mu$ M] (95% CI)	Hill slope	Hill R <sup>2</sup>	power constant ( $k_1$ ) = $\log t + \alpha \log C$		power R <sup>2</sup>	log- additive constant ( $K_2$ ) = $\log t + \log C$	log- additive R <sup>2</sup>
						$k_1$	$\alpha$			
1	>100	>100	>100	ND	ND	ND	ND	ND	ND	ND
2	7.6 (5.7 to 10)	1.2 (0.90 to 1.6)	0.28 (0.21 to 0.38)	0.71	1.0	2.1	0.98	0.98	2.1	0.98
3	>100	79 (73 to 85)	23 (19 to 27)	2.0	1.0	4.0	1.2	1.0	3.6	0.97
4	>100	>100	43 (40 to 47)	2.4	1.0	3.9	0.92	0.95	4.1	0.94
5	0.043 (0.035 to 0.054)	0.030 (0.023 to 0.037)	0.024 (0.019 to 0.031)	1.3	1.0	-5.2	4.7	0.97	0.28	0.37
6	13 (6.4 to 28)	3.9 (1.8 to 8.4)	1.3 (0.59 to 2.9)	0.65	0.99	2.5	1.2	1.0	2.4	0.97
7	2.8 (2.0 to 3.8)	1.5 (1.1 to 2.0)	0.58 (0.43 to 0.79)	0.85	1.0	2.0	1.7	0.98	1.9	0.80
8	4.1 (2.2 to 7.6)	2.3 (1.2 to 4.4)	1.5 (0.81 to 2.6)	1.1	0.99	2.8	2.7	1.0	2.2	0.60
9	0.037 (0.026 to 0.054)	0.023 (0.016 to 0.032)	0.0084 (0.0060 to 0.012)	0.90	0.99	-1.3	1.8	0.97	0.064	0.78
10	0.057 (0.048 to 0.066)	0.037 (0.031 to 0.044)	0.018 (0.015 to 0.021)	1.0	1.0	-1.7	2.4	0.98	0.31	0.65
11	0.031 (0.026 to 0.038)	0.026 (0.021 to 0.031)	0.012 (0.010 to 0.015)	0.83	1.0	-2.6	2.6	0.90	0.11	0.55
12	1.5 (0.69 to 3.5)	0.23 (0.10 to 0.53)	0.051 (0.023 to 0.120)	0.85	0.97	1.3	0.81	1.0	1.2	0.94
13	0.54 (0.22 to 1.3)	0.11 (0.044 to 0.27)	0.020 (0.0079 to 0.050)	0.84	0.95	0.96	0.84	1.0	0.80	0.96
14	0.77 (0.52 to 1.1)	0.20 (0.14 to 0.31)	0.056 (0.038 to 0.084)	0.91	0.99	1.1	1.1	1.0	1.1	1.0